

IEICE Proceeding Series

Experimental Investigation of Dynamical Scenarios of A Dual-beam
Optically Injected Semiconductor Laser

Yi-Huan Liao, Fan-Yi Lin

Vol. 1 pp. 207-210

Publication Date: 2014/03/17

Online ISSN: 2188-5079

Downloaded from www.proceeding.ieice.org

Experimental Investigation of Dynamical Scenarios of A Dual-beam Optically Injected Semiconductor Laser

Yi-Huan Liao and Fan-Yi Lin[†]

Institute of Photonics Technologies, Department of Electrical Engineering,
 National Tsing Hua University, Hsinchu 30013, Taiwan

[†] Email: fylin@ee.nthu.edu.tw

Abstract—We experimentally investigate different dynamical scenarios of a dual-beam optically injected semiconductor laser. The dynamical scenarios are differentiated by determining whether the nonlinear dynamics induced with each single beam alone is preserved (P), shifted (S), suppressed (S') or if injection locking has occurred (L). Dynamical scenarios of PP, PS, SP, SS, S'S', LS', S'L and LL are identified in the mappings under the injection strengths domain and the detuning frequencies domain, respectively. Transitions among different dynamical scenarios are also shown through comparing the oscillation frequencies of the slave laser subject to single-beam and dual-beam injections.

1. Introduction

Optically injected semiconductor lasers have been widely investigated in recent years. Rich nonlinear dynamics such as stable locking, periodic oscillations, and chaotic oscillation can be found by altering the injection strength and the detuning frequency between the master laser and the slave laser [1]. Each nonlinear dynamics has its own potentials in different applications. For example, the stable locking phenomenon under strong injection strength can enhance the microwave modulation bandwidth [2]. The period one (P1) state with dual-frequencies can be used as the light source of the Doppler velocimeter to reduce the speckle effect in detection [3]. The chaotic oscillation with broad bandwidth can be used as the light source of the lidar to eliminate the ambiguity [4].

The nonlinear dynamics of an optically injected semiconductor laser will become more complicated when it is injected by more than one optical beams [5]. Torger *et al.* studied a single-mode diode laser subject to external lights injection from several lasers [6]. Al-Hosiny *et al.* found a secondary locking region [7] and the tailoring enhanced chaos [8] in a two beam injected laser diode sequentially. Recently, Li *et al.* used the medium-gain model to explain the frequency-pushing effect in a dual-beam injected laser diode [9]. In order to address the competitions of the dynamics in a dual-beam optically injected semiconductor laser, Qi and Liu theoretically identified the dynamical scenarios [10].

In this paper, we experimentally investigate the dynamical

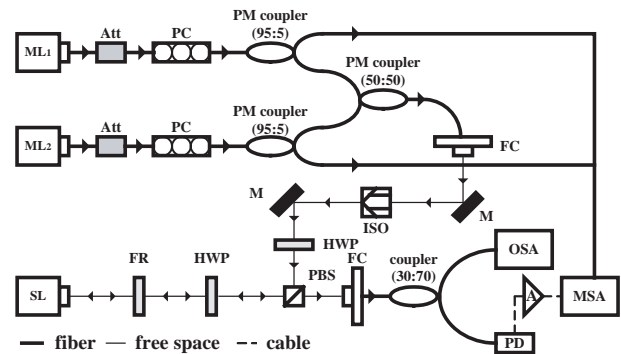


Fig. 1 Experimental setup of the dual-beam optical injection system. Att: attenuator, PC: polarization controller, PM: polarization-maintaining, FC: fiber coupler, M: mirror, ISO: isolator, HWP: half-wave plate, PBS: polarizing beam splitter, FR: Faraday rotator, OSA: optical spectrum analyzer, MSA: microwave spectrum analyzer, A: electronic amplifier PD: photodetector.

ical scenarios of a dual-beam optically injected semiconductor laser. The experimental setup and the operation conditions are shown in the next section. Following is the experimental results including the optical and electrical spectra of different scenarios, the mappings, and the transition among scenarios. The final section is the conclusions.

2. Experimental Setup

Figure 1 shows the experimental setup of the dual-beam optical injection system. Two tunable lasers (Yenista, Tunics-T100S, O-band) are used as the master lasers, ML_1 and ML_2 . A distributed-feedback (DFB) semiconductor laser (CYOPTICS, TO293BU-ADZ) is used as the slave laser, SL. The temperature and injection current of the SL are adjusted by a current-temperature controller (Newport, 8008). The wavelength of the SL is $\lambda_{SL} = 1309.029$ nm, which is controlled by the temperature of the SL with a ratio of 0.08 nm/K. The injection current of the SL is 10 mA ($1.2I_{th}$).

The injection strengths (defined as the ratio of the laser field amplitude between master lasers and slave laser) of ML_1 and ML_2 are adjusted by the attenuators. The

wavelengths and output powers of two injected beams are monitored from the 5 percent ports of two polarization-maintaining couplers (95:5). In order to confirm the ratio of these two beams injected into the SL, they are combined by another polarization-maintaining coupler (50:50). The combined dual-beam is coupled to free space and injected into the SL through a free space circulator. An isolator is used to confirm the unidirectional optical injection. The output of the SL is coupled into the fiber and divided into two parts. One part is sent to the optical spectrum analyzer (ADVANTEST, Q8384); the other part is detected by a photodetector (Discovery Semiconductor, DSC30S). The converted electronic signal from the photodetector is amplified by an electronic amplifier (MITEC, AFS5-00102000-30-10P-6) and sent to the microwave spectrum analyzer (Agilent, E4407B).

3. Experimental Results and Discussions

3.1. Scenarios of the nonlinear dynamics

For a traditional optical injection system, the carrier density in the SL will be depleted by the injected light. This induces the red-shift in the frequency of free-running laser of the SL. The amount of the frequency shift of the SL can be described as $\Delta f_{shift} = \alpha G_N \Delta N / 2$, where α is the linewidth enhancement factor, G_N is the differential gain, and N is the carrier density. Hence, the oscillation frequency of the SL is given by $f_r^{single} = |f - \Delta f_{shift}|$, where f is the detuning frequency between the ML and the SL. The oscillation frequency is one of the characteristics of the nonlinear dynamics which depends on the injection strength and the detuning frequency. In the dual-beam optical injection system, the output of the SL has three main frequency lines in the optical spectra, i.e. ν_{ML_1} from the ML₁, ν_{ML_2} from the ML₂, and ν_{SL} from the red-shift of the SL. In this case, there are two oscillation frequencies: $f_{r,1}^{dual}$ is the beat frequency between ν_{ML_1} and ν_{SL} , and $f_{r,2}^{dual}$ is the beat frequency between ν_{ML_2} and ν_{SL} . The oscillation frequencies of the SL subject to dual beam injections ($f_{r,1}^{dual}$ and $f_{r,2}^{dual}$) are used to compare with those subject to single beam injections ($f_{r,1}^{single}$ and $f_{r,2}^{single}$). We define that the dynamics induced with single beam injection is preserved (P) if $(f_{r,1}^{dual} - f_{r,1}^{single}) / f_{r,1}^{single} \leq 1\%$ or $(f_{r,2}^{dual} - f_{r,2}^{single}) / f_{r,2}^{single} \leq 1\%$, shifted (S) if $(f_{r,1}^{dual} - f_{r,1}^{single}) / f_{r,1}^{single} > 1\%$ or $(f_{r,2}^{dual} - f_{r,2}^{single}) / f_{r,2}^{single} > 1\%$, suppressed (S') if the magnitude of $f_{r,1}^{dual}$ or $f_{r,2}^{dual}$ is below the noise level of -65 dBm in the power spectrum and locked (L) if the SL is injection locked with the ML₁ or ML₂ originally.

Figures 2(a)-2(e) show the optical spectra of scenarios PP, PS, SS, S'S', and S'L, respectively. The red line (ML₁) and the blue line (ML₂) are the single-beam injections and the black line is the dual-beam injection. Figures 2(f)-2(j) are the corresponding power spectra of Figs. 2(a)-2(e). For Fig. 2(f) ($\xi_1, f_1, \xi_2, f_2 = 0.283, 15.06 \text{ GHz}, 0.4, 20.84$

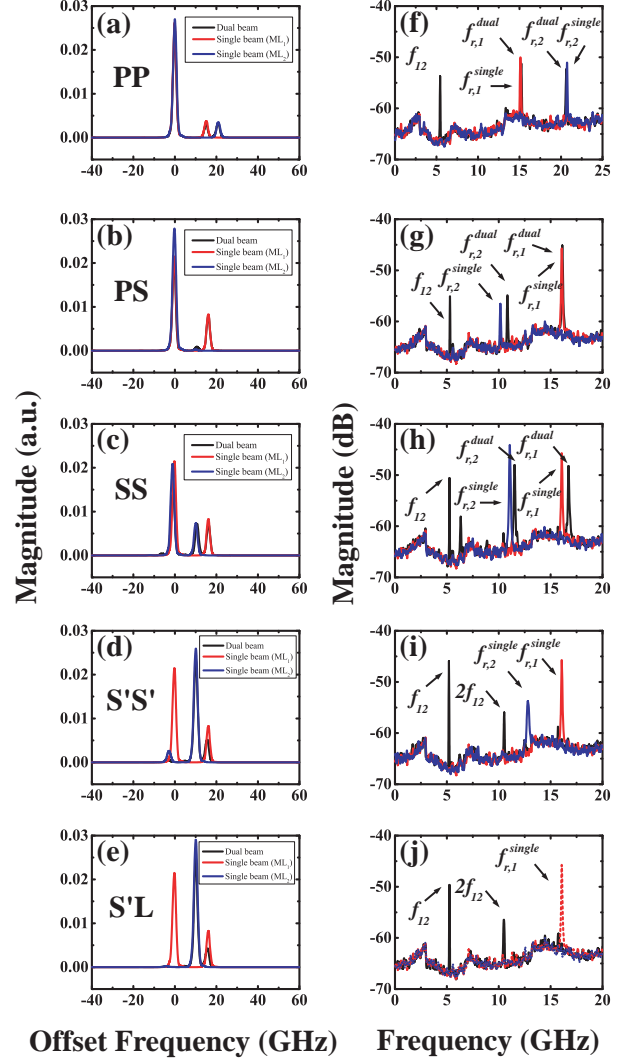


Fig. 2 (a)-(e) Optical spectra and (f)-(j) their corresponding power spectra of the scenarios PP, PS, SS, S'S', and S'L. Red line (ML₁) and blue line (ML₂) are the single-beam injections and black line is the dual-beam injection.

GHz), $f_{r,1}^{dual}$ and $f_{r,2}^{dual}$ equal to $f_{r,1}^{single}$ and $f_{r,2}^{single}$. The dynamics induced with each single-beam optical injection are preserved. It is the scenario PP. For Fig. 2(g) ($\xi_1, f_1, \xi_2, f_2 = 0.456, 15.8 \text{ GHz}, 0.055, 10.3 \text{ GHz}$), $f_{r,1}^{dual}$ equals to $f_{r,1}^{single}$ but $f_{r,2}^{dual}$ has a shift from $f_{r,2}^{single}$. The dynamics induced with ML₁ is preserved, whereas the dynamics induced with ML₂ is shifted. It is the scenario PS. If we increase ξ_2 to 0.311 and fix other parameters, both $f_{r,1}^{dual}$ and $f_{r,2}^{dual}$ have shifts from $f_{r,1}^{single}$ and $f_{r,2}^{single}$. As shown in Fig. 2(h), the dynamics induced with each single-beam optical injection are shifted. It is the scenario SS. If we increase ξ_2 further to 0.641 and fix other parameters, both $f_{r,1}^{dual}$ and $f_{r,2}^{dual}$ decrease below the noise level. As shown in Fig. 2(i), the cavity resonance frequency of ν_{SL} is significantly suppressed due to the draining of the gain in the SL, and the dynamics

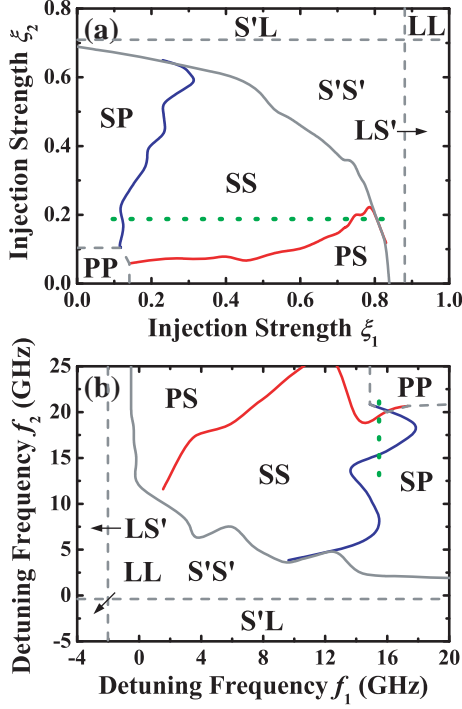


Fig. 3 Mappings of dynamical scenarios under different (a) injection strengths and (b) detuning frequencies. The detuning frequencies are fixed at $f_1 = 15.8$ GHz and $f_2 = 10.3$ GHz in (a) and the injection strengths are fixed at $\xi_1 = 0.283$ and $\xi_2 = 0.4$ in (b).

of dual-beam optical injection system is dominated by the beat frequency of $f_{12} = |v_{ML_1} - v_{ML_2}|$ and its harmonics. It is the scenario S'S'. If ξ_2 is increased over the stable locking boundary ($\xi_2, f_2 = 0.707, 10.3$ GHz), $f_{r,2}^{single}$ does not exist and can not be used as the reference in determining the changes between $f_{r,2}^{dual}$ and $f_{r,2}^{single}$. So, the S'L is used to separate this originally injection-locked scenario from the previously introduced S'S' scenario. For the same reason, scenarios LS' and LL means that the SL is originally injection-locked by the ML_1 or by both the ML_1 and ML_2 , respectively.

Figures 3(a) shows the mapping of the dynamical scenarios as a function of dual-beam injection strengths. The detuning frequencies of the ML_1 and ML_2 are fixed at $f_1 = v_{ML_1} - v_{SL} = 15.8$ GHz and $f_2 = v_{ML_2} - v_{SL} = 10.3$ GHz. For the left-lower corner region, both of the dual-beam injection strengths are small. The cavity resonant frequency of the SL does not red-shift (same as the frequency of free-running laser) due to the dual-beam injections. Hence both of the oscillation frequencies originally induced with single-beam injections are preserved in the dual-beam injections. It is scenario PP. When we increase one of the dual-beam injection strengths, the cavity resonant frequency of the SL start to red-shift. The amount of the shift is dominated by the stronger beam, so one of the oscillation frequencies originally induced with single-beam injections

is preserved and the other is shifted. They are scenarios PS and SP located at lower and left regions, respectively. When both of the dual-beam injection strengths strong enough to contribute to the red-shift in the cavity resonant frequency of the SL, both of the oscillation frequencies originally induced with single-beam injections are shifted in the dual-beam injections. It is scenario SS located at the middle region between scenario PS and SP. Further increasing the dual-beam injection strengths causes the gain draining in the cavity resonant frequency of the SL, both of the oscillation frequencies originally induced with single-beam injections are suppressed in the dual-beam injections. It is scenario S'S' located at the right-upper side of scenario SS. When one or both of the dual-beam injection strengths exceed the stable locking boundary ($\xi_1 = 0.883, \xi_2 = 0.707$), the oscillation frequencies originally induced with single-beam injections do not exist. We use the scenarios LS', S'L, and LL to separate them from the S'S' scenario.

Figures 3(b) shows the mapping of the dynamical scenarios as a function of dual-beam detuning frequencies. The injection strengths of the ML_1 and ML_2 are fixed at $\xi_1 = 0.283$ and $\xi_2 = 0.4$. Because the effect to the SL are opposite between the injection strengths and the detuning frequencies, each scenario is located at the opposite position between Fig. 3(a) and Fig. 3(b). For example, the scenario PP region is located at the left-lower corner of small injection strengths in Fig. 3(a) but it is located at the right-upper corner of large detuning frequencies in Fig. 3(b). Instead of abrupt boundaries between the scenarios, the SL gradually emerges into different scenarios as the controlled parameters vary.

3.2. Transition among scenarios

The transitions among different scenarios can be found by observing the oscillation frequencies of SL subject to dual-beam injection, $f_{r,1}^{dual}$ and $f_{r,2}^{dual}$, and single-beam injection, $f_{r,1}^{single}$ and $f_{r,2}^{single}$, simultaneously. Figures 4(a) shows the oscillation frequencies as a function of ξ_1 which is marked as the green dotted line in Fig. 3(a). The other parameters are $\xi_2 = 0.197, f_1 = 15.8$ GHz, and $f_2 = 10.3$ GHz. For $\xi_1 < 0.141$, $f_{r,1}^{dual}$ deviates from $f_{r,1}^{single}$, but $f_{r,2}^{dual}$ coincides with $f_{r,2}^{single}$, which is the scenario SP. When ξ_1 increases over 0.141, $f_{r,2}^{dual}$ starts to depart from $f_{r,2}^{single}$. A transition from scenario SP to scenario SS is occurred. When ξ_1 increases to 0.735, $f_{r,1}^{dual}$ closes to $f_{r,1}^{single}$. A transition from scenario SS to scenario PS is occurred. When ξ_1 increases over 0.796, both $f_{r,1}^{dual}$ and $f_{r,2}^{dual}$ disappear. The SL goes into the scenario S'S'.

Figures 4(b) shows the resonance frequencies as a function of f_2 which is marked as the green dotted line in Fig. 3(b). The other parameters are $\xi_1 = 0.283, \xi_2 = 0.4$, and $f_1 = 15.06$ GHz. In the regions of 12 GHz $< f_2 < 13.13$ GHz and 19.6 GHz $< f_2 < 21$ GHz, $f_{r,2}^{dual}$ coincides with $f_{r,2}^{single}$. It means the dynamics induced with ML_2 is

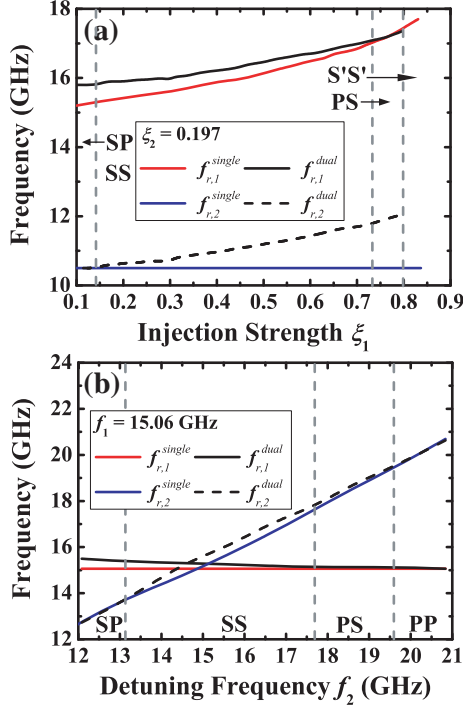


Fig. 4 Oscillation frequencies of the SL subject to single-beam and dual-beam injections when (a) ξ_1 and (b) f_2 vary. The injection parameters used in (a) and (b) are chosen to represent the green dotted lines marked in Figs. 3(a) and (b), respectively, where the transitions among different scenarios are traced.

preserved (P). In the region of $13.13 \text{ GHz} < f_2 < 19.6 \text{ GHz}$, $f_{r,2}^{dual}$ deviates from $f_{r,2}^{single}$. It means the dynamics induced by ML_2 is shift (S). For the same reason, the dynamics induced by ML_1 is preserved (P) in the region of $17.68 \text{ GHz} < f_2 < 21 \text{ GHz}$, but is suppressed (S) in the region of $12 \text{ GHz} < f_2 < 17.68 \text{ GHz}$. Combining the preserved and shifted regions of ML_1 and ML_2 , we can find the scenarios SP, SS, PS, and PP with the transition points of $f_2 = 13.13 \text{ GHz}$, 17.68 GHz , and 19.6 GHz , respectively.

4. Conclusions

In this work, we experimentally study the dynamical scenarios of a dual-beam optically injected semiconductor laser. The nonlinear dynamics of the SL induced with single-beam optical injection can be preserved, shifted, suppressed or originally locked when another beam is injected into the SL simultaneously. Scenarios PP, PS, SP, SS, S'S', S'L, LS', and LL are defined and the mappings of these scenarios in the parameter space are plotted. Transitions among different scenarios are investigated by observing the changes of the oscillation frequencies of SL under dual-beam injection and single-beam injection.

Acknowledgments

This work is supported by the National Science Council of Taiwan under contract NSC-100-2112-M-007-012-MY3 and National Tsing Hua University under grant 100N-7081E1.

References

- [1] F. Y. Lin, S. Y. Tu, C. C. Huang, and S. M. Chang, "Nonlinear dynamics of semiconductor lasers under optical repetitive pulse injection," *J. of Sel. Top. Quantum Electron.*, vol.15, pp.604–611, 2009.
- [2] J. M. Liu, H. F. Chen, X. J. Meng, and T. B. Simpson, "Modulation bandwidth, noise, and stability of a semiconductor laser subject to strong injection locking," *IEEE Photon. Technol. Lett.*, vol.9, pp.1325–1327, 1997.
- [3] C. H. Cheng, J. W. Lee, T. W. Lin, and F. Y. Lin. "Speckle noise reduction of a dual-frequency laser Doppler velocimeter based on an optically injected semiconductor laser," *Proc. of SPIE*, vol.8255, 82551p1–82551p6, 2012.
- [4] W. T. Wu, Y. H. Liao, and F. Y. Lin, "Noise suppressions in synchronized chaos lidars," *Opt. Express*, vol.18, pp.26155–26162, 2010.
- [5] Y. S. Juan and F. Y. Lin "Photonic generation of broadly tunable microwave signals utilizing a dual-beam optically injected semiconductor laser," *IEEE Photonics J.*, vol.3, pp.644–650, 2011.
- [6] J. Torger, L. Thevenaz, P. A. Nicati and P. A. Robert, "Theory and experiment of a single-mode diode laser subject to external light injection from several lasers," *IEEE J. Lightwave Technol.*, vol.17, pp.629–639, 1999.
- [7] N. Al-Hosiny, I. D. Henning, and M. J. Adams, "Secondary locking regions in laser diode subject to optical injection from two lasers," *Electron. Lett.*, vol.42, pp.759–760, 2006.
- [8] N. Al-Hosiny, I. D. Henning, and M. J. Adams, "Tailoring enhanced chaos in optically injected semiconductor lasrs," *Opt. Commun.*, vol.269, pp.166–173, 2007.
- [9] W. Li, N. H. Zhu, L. X. Wang, J. H. Ke, S. F. Chen, X. Q. Oi, B. H. Zhang and L. Xie, "Frequency-pushing effect in single-mode diode laser subject to external dual-beam injection," *IEEE J. Quantum Electron.*, vol.46, pp.796–803, 2010.
- [10] X. Q. Qi and J. M. Liu, "Dynamics scenarios of dual-beam optically injected semiconductor lasers," *IEEE J. Quantum Electron.*, vol.47, pp.762–769, 2011.